QUIET: Ensuring the Efficacy of Damping Systems for Cryogenic Dark Matter and Rare Event Searches

Sara Earnest

Department of Physics and Astronomy, Johns Hopkins University, 3400 N. Charles Street, Baltimore, Maryland 21218, USA

searnes1@alumni.jh.edu

Abstract. It is a common problem in detector physics that reducing noise of one type introduces noise from another source, lowering the practical sensitivity of detector instruments. This investigation is an analysis of vibrational noise from around a pulse-tube-cooled dilution refrigerator (DR) intended to test instruments for particle dark matter and rare event searches. Analysis of the frequencies of vibrational noise near the DR finds that the active vibrational damping used in the lab lowers the noise by more than 87.36% in the frequency band between 6 and 19 Hz, which is where the cooling system contributes the most significant mechanical noise.

INTRODUCTION

This work addresses a complex question in two parts. First, for sensitive, cryogenic rare event searches, how can we characterize vibrational noise from the cooling system? And second, how can we determine whether existing systems to mitigate such noise are effective? These questions are important, as ground-based cryogenic experiments for low energy measurements require extremely sensitive detectors to resolve very weak signals [1, 2]. However, in being so sensitive, these detectors also pick up a significant amount of noise from their environment. For example, in cryogenically cooling cavities to reduce thermal noise, vibrational noise is introduced through the instruments that comprise the cooling system. As a result, the accuracy of such a system's signal readout is heavily impacted by the efficacy of vibrational damping systems, and it becomes necessary to confirm and qualify the efficacy of that damping system.

The Johns Hopkins laboratory where we conducted this work uses an LD400 BlueFors dilution refrigeration (DR) system [3] to test microwave cavities along with semiconductor and superconducting material samples at millikelvin temperatures in support of dark matter and rare event searches conducted in other laboratories, including the HAYSTAC, ALPHA, CUORE, and CUPID experiments. It is also set up to do detector research and design. The ability to accurately identify low-frequency vibrational noise in the lab environment supports the HAYSTAC experiment in particular. The presence of mechanical noise at frequencies under 200 Hz [4] can directly interfere with instruments like Josephson parametric amplifiers (JPAs) [5] that are used to enhance the sensitivity of detectors looking for axion signals by mitigating the noise from fundamental quantum uncertainty [5].

The cooling process for the DR introduces consistent vibrational noise at mid-to-low frequencies through the use of pulse tubes to precool the 3-He before it is circulated through the system [6]. A more detailed discussion of dry dilution refrigerators can be found in Pobell's *Matter and Methods at Low Temperatures* [7]. In addition to the DR, the laboratory uses a heavy frame for passive vibrational damping, as well as a Table Stable AVI-200XL/LP active damping system [8]. The combination of active and passive damping was intended to reduce vibrational noise in the experimental payload primarily over the 6–20 Hz frequency range, and thus in this work we sought to not only identify the DR's noise environment but also to ensure the damping systems worked as intended.

THE EXPERIMENT

As mentioned, this lab uses an active vibrational damping system to mitigate mechanical noise. For this experiment, we used an accelerometer to record this noise and wrote a script in MATLAB to take its power spectral density to characterize which frequencies were most prominently introduced by the DR cooling system. The accelerometer is a PCB Piezoelectronics model 393B04 and is sensitive to vibrations between 0.06 and 450 Hz [9]. Both the damping system and the accelerometer are mounted on the scaffolding that holds up the dilution refrigerator (see Fig. 1). This placement of the accelerometer was chosen because from there it can easily detect noise from the pulse tubes without having to be inside the cavity itself. See the Table Stable website for more detail on the damping system specifications

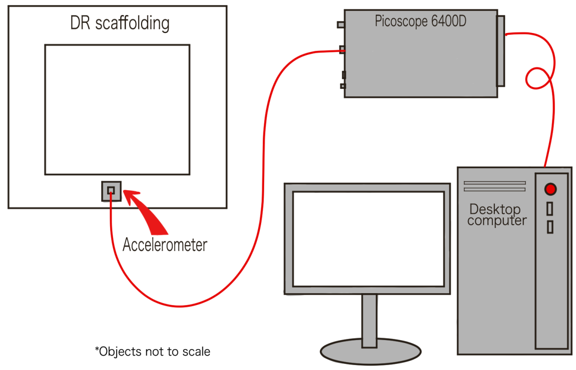

FIGURE 1: A schematic showing the connection path of the accelerometer to the picoscope and desktop computer used to export vibration data for processing.

[8]. The heavy passive frame of the DR acts as a stable base on the laboratory floor, while the active damping units sit directly between this frame and the scaffolding that holds up the dilution refrigerator. This configuration places the active system right in the path of the pulse tube vibrations, allowing it to absorb and cancel the mechanical noise before it can shake the experimental setup. The accelerometer data were digitized using a PicoScope 6404D PC oscilloscope and exported as time-series voltage vectors for spectral processing [10]. We then used the MATLAB code we wrote to generate a power spectral density from the data. The script was coded to use the accelerometer signal output (which is exported as segmented waveforms of a continuous dataset) to stitch the data together into a continuous time history and use user-selected, power-of-two window segments to balance frequency resolution against background noise variance. It also calculates the mean sampling frequency and from these items computes the final power spectral density curves. The accuracy of the MATLAB processing script was successfully verified prior to data analysis by resolving a clean, single peak from a 100-Hz calibration signal generator.

THE PSD MODEL

The power spectral density (PSD) is a tool that allows the user to clearly see the intensity of recurring frequencies of a continuous signal—in this case, that signal is vibrational noise. While a standard power spectrum measures discrete power at specific frequencies, a power spectral density characterizes how the power of a random, continuous signal is distributed over a continuous frequency spectrum per unit of bandwidth [11]. Using a spectral density rather than a raw spectrum allows us to make accurate, normalized comparisons of random vibration signals with different total recording lengths [11]. The power spectrum of a time-dependent function $x(t)$ is defined from the Fourier transform:

$$S_{xx}(f) = \lim_{T\to\infty} \frac{1}{T} |\hat{x}_T(f)|^2, \tag{1}$$

where $\hat{x}_T(t) = \int_{-\infty}^{\infty} e^{-i2\pi ft} x(t)$.

Here, $x(t)$ is defined in terms of a voltage with time history units of mV/s. Because there is no unique electrical impedance associated with the open-circuit sensor layout, physical "power" is conventionally reckoned in terms of the square of the voltage signal, which remains directly proportional to the true mechanical energy of the vibrations [11]. Generally, the units of a PSD will be the ratio of units of variance per unit of frequency. For example, the power spectrum of this series of voltages (in milliVolts) over time (in seconds) has units of mV^2/Hz.

To quantify the total vibrational energy contained within a specific frequency band (such as the target 6–19 Hz window), the PSD of the voltage signal, denoted as $S_{xx}(f)$, must be integrated over that frequency interval,

$$V_{\text{band}}^2 = \int_{f_1}^{f_2} S_{xx}(f)df. \tag{2}$$

Multiplying the spectral density ($\mathrm{mV}^2/\mathrm{Hz}$) by the differential frequency width (df, in hertz) cancels the frequency dimension, yielding the total mean-square voltage (V_{band}^2) in units of mV^2. Taking the square root of this integrated value yields the band-limited root-mean-square (RMS) amplitude [11]:

$$V_{\mathrm{RMS}} = \sqrt{\int_{f_1}^{f_2} S_{xx}(f)df}. \tag{3}$$

This operation returns the final metric to a linear physical dimension of millivolts and provides the dimensionality used to construct the comparative baseline analyses presented in Fig. 2(b).

DATA AND RESULTS

Figure 2 shows the PSD for all four operational configurations. Without the pulse tubes (PT) or damping system running, the baseline noise level is low and generally flat. Engaging the active damping system introduces a minor increase in noise below 6 Hz compared to the undamped signal, with a slight bulge in amplitude between 4 and 5 Hz with the the PT off. This is a side effect of the table's feedback loop known as the "waterbed effect" [8, 12] (a full description of which can be found in [12]). However, this is not considered disruptive for experiments like HAYSTAC, as it can be handled by the detector's internal tuning systems [5]. In contrast, the 6–20 Hz vibrations from the cooling system directly shake the cavity. Thus, the damping system is considered especially successful if it reduces these sharp peaks up to 20 Hz down toward the laboratory's baseline noise level.

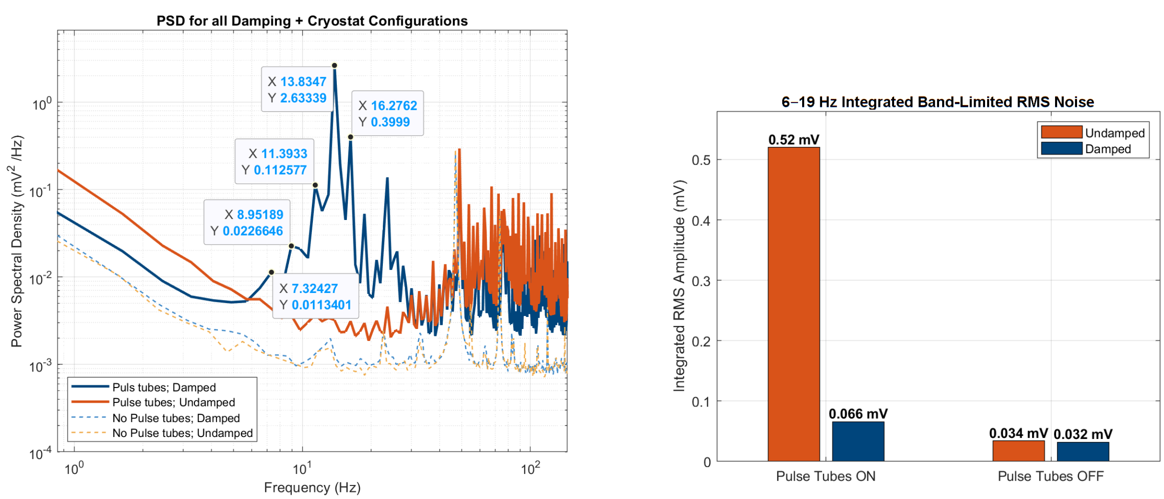

(a)

(b)

FIGURE 2: (a) Log-scale power spectral density (PSD) of environmental vibrational noise measured at the dilution refrigerator scaffolding across all four permutations of pulse tube (PT) and active damping operation. (b) Visual representation of the 87.36% total reduction in band-limited RMS acceleration amplitude achieved within the critical 6–19 Hz frequency band, compared with the baseline RMS amplitude when the pulse tubes are off.

The data compared here were acquired during the same testing phase under identical signal processing configurations. Because the DR needs time to thermally stabilize when turning cooling subsystems on or off, data isolating the active pulse tube states (PT On) and the unexcited environmental baselines (PT Off) were recorded on separate days. However, within each respective day's observation window, conditions were separated chronologically only by the time required to toggle the active damping table (less than 5 min). In all cases, vibration data were recorded continuously at a sampling rate of 2000 Hz across five sequential blocks, but spectral processing was performed over the full continuous run. Consequently, all configurations of noise environment conditions shown in Fig. 2 utilize an identical total integration time of 163.84 s (1.64×10^5 ms). Utilizing Welch's method with a rectangular window, a segment length of 4096 samples, and 50% overlap, this expanded dataset yielded 159 independent segments for ensemble averaging to lower the statistical variance of the baseline noise floor.

Beyond a threshold of about 6 Hz, the undamped, active cryocooler spectrum (PT On, Damping Off) is heavily dominated by a dense cluster of intermediate peaks separated by about 2.5 Hz, labeled in Fig. 2(a) at 7.3, 8.9, 11.4, 13.8, and 16.3 Hz. Comparing this profile to the baseline state (PT Off, Damping Off) confirms that these distinct peaks are not ambient facility noise but rather the result of the natural structural resonances of the cryostat's metal frame and the rhythmic pulsing of the helium compressor. As demonstrated by the integrated band analysis in Fig. 2(b), the active damping system successfully suppresses this entire cluster of induced modes, reducing the total band-limited RMS noise within the 6–19-Hz region by 87.36% (from 0.5201 mV to 0.0657 mV) and returns the vibrational noise level near the cryostat remarkably close to its fundamental unexcited baseline of 0.0338 mV within that frequency band. Additionally, if we take into account frequencies from 1 to 200 Hz (the band which is of particular concern for the use of JPAs in the HAYSTAC experiment [4]), we continue to see noise attenuation with the pulse tubes on up to about 22%.

CONCLUSION

The power spectra obtained from this investigation are useful for understanding the vibrational noise environment near the DR in this cryogenic test laboratory and how well the current damping system reduces vibrational noise. We found a clear reduction in noise at the harmonics of the natural forcing frequency of the pulse tubes when using the damping system. With the vibrational noise environment characterized, the combination of active and passive damping employed in this laboratory is confirmed to be effective in mitigating this noise at the higher harmonics of the pulse tube signal, suppressing almost entirely peak resonances in the undamped signal, specifically reducing noise in the 6–19 Hz frequency band by 87.36%. Verifying that noise in this specific frequency band can be heavily mitigated using the current combined isolation methodology provides a critical, quantified benchmark for ongoing detector optimization and signal readout accuracy. Additionally, as the MATLAB script used to analyze the accelerometer data is saved within the laboratory computers, similar analyses can be completed easily with future noise measurements.

ACKNOWLEDGMENTS

Many thanks to Johns Hopkins associate physics professor Danielle Speller for her advice and mentoring, and to the members of her Speller Lab for providing a supportive environment for me to conduct this work as an undergraduate.

REFERENCES

1. P. Sikivie, "Invisible axion search methods," Rev. Mod. Phys. **93**, 015004 (2021).
2. A. J. AMillar, S. M. Anlage, R. Balafendiev, P. Belov, K. van Bibber, J. Conrad, M. Demarteau, A. Droster, K. Dunne, A. G. Rosso, et al., "Searching for dark matter with plasma haloscopes," Phys. Rev. D **107**, 055013 (2023).
3. BF-LD-SERIES, *BF-LD-SERIES CRYOGEN-FREE DILUTION REFRIGERATOR SYSTEM: User Manual*.
4. X. Bai, M. Jewell, J. Echevers, K. van Bibber, A. Droster, M. H. Esmat, S. Ghosh, E. Graham, H. Jackson, C. Laffan, et al., "Dark matter axion search with HAYSTAC phase II," Phys. Rev. Lett. **134** (2025).
5. K. M. Backes, D. A. Palken, S. A. Kenany, B. M. Brubaker, S. B. Cahn, A. Droster, G. C. Hilton, S. Ghosh, H. Jackson, S. K. Lamoreaux, et al., "A quantum enhanced search for dark matter axions," Nat. **590**, 238–242 (2021).
6. Bluefors, "How does a dilution refrigerator work?" Bluefors Newsletter (2023).
7. F. Pobell, *Matter and Methods at Low Temperatures, 3rd ed.* (Springer-Verlag, Berlin Heidelberg, 2007).
8. Table Stable, ABI-200LP Manual, *Active Vibration Isolation System AVI-200 LP: Instruction Manual*.
9. Model 393B04, *PCB Piezotronics, Inc. Model 393B04 Seismic, miniature (50 gm), ceramic flexural ICP® accel., 1 V/g, 0.06 to 450 Installation and Operating Manual*.
10. Picoscope 6000 Series, *Picoscope 6000 Series PC Oscilloscopes (A, B, C, and D Models): User's Guide*.
11. A. V. Oppenheim and G. Verghese, *Signals, Systems & Inference* (Pearson, London, 2016).
12. A. Megretski, "The waterbed effect," MIT OpenCourseWare, Lecture Notes for 6.245: Multivariable Control Systems (2004), MIT.